Organic & Biomolecular Chemistry

ROYAL SOCIETY OF CHEMISTRY

PAPER

View Article Online
View Journal

Cite this: DOI: 10.1039/d0ob00938e

Multi-stimuli controlled release of a transmembrane chloride ion carrier from a sulfonium-linked procarrier†

Sribash Das,‡ Oindrila Biswas,‡ Nasim Akhtar, Anjali Patel and Debasis Manna *

Received 6th May 2020,
Accepted 27th October 2020

DOI: 10.1039/d0ob00938e

rsc.li/obc

In recent times, anion transporters have received substantial consideration due to their ability to disrupt the ionic equilibrium across membrane bilayers. While numerous Cl^- ion transporters were developed for channelopathies, unfortunately, poor aqueous solubility precluded their bioapplicability. Herein, we demonstrate the development of a multi-stimuli activatable anion transport approach to induce regulated transport of Cl^- ions across membranes under specific conditions. The sulfonium-based procarrier was initially inactive, but the transmembrane transport of Cl^- ions was activated in the presence of stimuli such as glutathione (GSH), reactive oxygen species (ROS) and light. The release of the hydrophobic anionophore from the aqueous-soluble procarrier under specific conditions leads to the successful transport of Cl^- ions. Under physiological conditions, these anion carriers follow an antiport exchange mechanism to transport Cl^- ions across lipid bilayers. Such multi-stimuli activatable procarriers have great potential to combat various types of channelopathies, including cancer, cystic fibrosis, kidney stones, myotonia, and others.

Introduction

Multicellular organisms promote cell proliferation and eliminate potentially harmful cells to maintain tissue homeostasis. However, disorders in apoptotic pathways are linked to neurodegenerative disorders, cancer, and other diseases. Cancer cells evade apoptosis even though they are under persistent stress stimuli such as oxidative stress and cellular hypoxia.[1–5] The oxidative stress allows the overproduction of reactive oxygen species (ROS) in the cell, which leads to mitochondrial dysfunction. Cancer cells also produce excess antioxidants such as glutathione (GSH) to minimize the effect of ROS and prevent oxidative stress-mediated apoptosis. However, the overproduction of GSH also allows cancer cells to develop drug resistance.[6] Therefore, the development of a new strategy that targets these overproduced ROS and GSH to induce apoptosis in cancer cells is highly beneficial.

Recent studies revealed that the apoptosis of cancer cells is also associated with the homeostasis of several ions, including potassium and chloride. In this regard, synthetic ionophores have been developed as potential anticancer agents.[4,5,7–18] Lipid-soluble synthetic ionophores catalyze the transport of ions across hydrophobic membranes to promote apoptosis. These molecules generally do not bind to any target specific proteins or genetic materials. Therefore, it is postulated that the synthetic ion transporters can overcome the resistance associated with the overexpression and mutations of genes and proteins. However, the lipophilicity of these synthetic ion carriers precluded their target specific cellular delivery and *in vivo* applications. Poor aqueous solubility is one of the reasons for the clinical trial failure of obatoclax, a Cl^- ion carrier and inhibitor of the Bcl-2 family of antiapoptotic proteins.[19–21] Therefore, an additional delivery system is required to accomplish the expected biological effects of these lipophilic ion carriers. Hence, a novel strategy is needed to mitigate the challenges of selective cellular uptake and target specific deliverability of hydrophobic anionophores.

Previously, we developed a stimuli-responsive Cl^- ion transport strategy for promoting controlled transport of Cl^- ions across lipid bilayers. We were successful in regenerating the lipophilic anionophores from water-soluble proanionophores after *in situ* cleavages of the hydrophilic accessories in the presence of glutathione (GSH).[19] Recently, this approach has been used for constructing ion-channels to induce cancer cell apoptosis. However, the poor aqueous solubility of the 2-hydroxyisophthalamide-based aninophore might be the main obstacle for its deliverability at the specific site and *in vivo* applications.[22] Previously, a nitrobenzyl-based cationic linker

Department of Chemistry, Indian Institute of Technology Guwahati, Assam 781039, India. E-mail: dmanna@iitg.ac.in

†Electronic supplementary information (ESI) available. See DOI: 10.1039/d0ob00938e

‡These authors contributed equally to this work.

was also used for improving the aqueous solubility of the hydrophobic estrogen receptor antagonist, tamoxifen.[23] Hence, stimuli-mediated alteration of the solubility of the ion transporters can be considered as one of the promising therapeutic approaches in cancer.

Herein, we introduce a GSH-, ROS-, and photo-responsive anion transport strategy to regenerate lipophilic anionophores from water-soluble proanionophores and promote controlled transport of Cl^- ions across lipid bilayers. The use of only external stimuli, such as light, has several limitations as it has lower tissue penetration ability.[24] The smaller change in the pH gradient between cancerous and normal cells may not be adequate for obtaining reliable *in vivo* results.[10,11,15] We hypothesize that this multi-stimuli-responsive anion transport strategy could be beneficial for targeting different types of cancer cells. The higher intracellular levels of GSH and ROS in cancer cells in comparison with those in normal healthy cells would preferentially release anionophores within the cancer cells, leading to the induction of apoptosis by perturbing the ion homeostasis. The GSH-mediated cleavage of sulfonium moieties is used in several applications, including drug delivery and selective protein and peptide modifications.[25–27] The installation of a sulfonium moiety also improves the viabilities and cellular uptake compared to other onium-based moieties and leads to facile reductive cleavage under physiological conditions.[25] The sulfonamide containing dipodal compounds showed chloride-mediated apoptosis-inducing activities in cancer cells.[8] Recently, we demonstrated the development of *S*-methylcysteamine-based thiourea containing dipodal compounds. However, its aggregation properties restricted its further applications.[19] We hypothesized that the installation of a 4-carboxy-2-nitrobenzyl sulfonium moiety would increase the aqueous solubility of the corresponding anionophore and allow its removal at high GSH and ROS concentrations or in the presence of light (Fig. 1A). Therefore, we installed a 4-carboxy-2-nitrobenzyl group linked *via* the sulfonium moiety, as the group is responsive to its linking to membrane-active anionophores. Substituted aryl groups were attached at the other end of the 1,3-phenylenedimethanamine scaffold to optimize the ion transport efficiency. The outcome of our studies revealed that the water-soluble proanionophores successfully release the membrane active ionophores in the presence of stimuli such as GSH, ROS, and light, which transport Cl^- ions across the model lipid bilayers.

Results and discussion

Compounds **1a–1d** were synthesized from 1-(3-(isothiocyanatomethyl)benzyl)-3-(2-(methylthio)ethyl)thiourea *via* condensation with the corresponding amines. The 4-carboxy-2-nitrobenzyl sulfonium appended compound **2** was synthesized by reacting compound **1c** with 4-bromomethyl-3-nitrobenzoic acid (Fig. 1B). Several thiourea-based dipodal ionophores have already been described,[8,19] but the presence of a methylthioethyl moiety allows these synthesized compounds to generate water-soluble proanionophores. All the synthesized compounds were purified by column chromatography and characterized by ^{1}H NMR, ^{13}C NMR, and HRMS analysis.

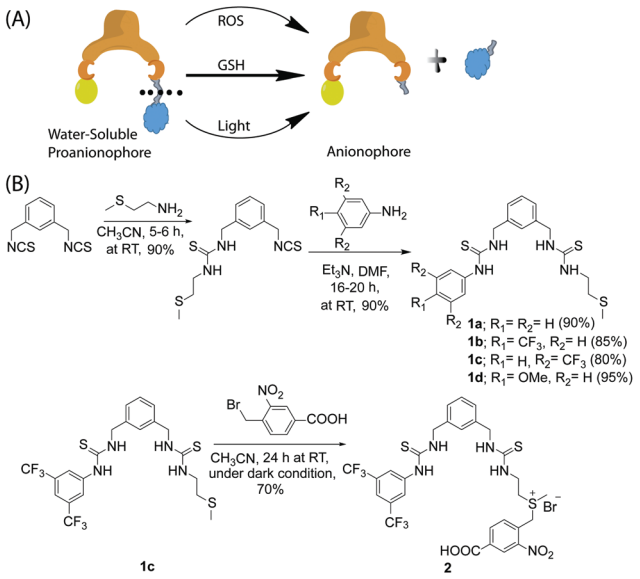

Fig. 1 Schematic diagram representing the stimuli-responsive release of an anionophore from its proanionophore (A). Synthesis of anionophores and proanionophores (B).

The ^{1}H NMR titration experiment was conducted to investigate the Cl^- ion recognition competence of the compounds.[7–10,19,22] Tetrabutylammonium chloride (TBACl) was used as the source of Cl^- ions. The downfield chemical shifts of N–H signals suggest the interaction of Cl^- ions with the compounds through hydrogen bonding. The strength of interactions was scrutinized by calculating the binding affinities (K_a) from the chemical shift ($\Delta\delta$) values for the N–H signals, using the BindFit v0.5 program. The inbuilt 1 : 1 binding model provided the best fit for the titration curves. The calculated K_a values revealed that compounds **1b** and **1c** have higher Cl^- ion binding capabilities (Table 1 and Fig. S1–4†). The ^{1}H NMR titration experiment was also performed in CD_3CN solvent to investigate the effect of the solvent on the Cl^- ion recognition properties of the compounds. The calculated K_a values of compound **1c** were 69.08 (Fig. S5†) and 105.21 M^{-1} (Fig. S3†) in DMSO-d_6 and CD_3CN

Table 1 Physical properties of the thiourea derivatives

Compound	Clog P^a	$K_a{}^b$ (M^{-1})	$EC_{50}{}^c$ (μM) (n)
1a	4.18	32.07 ± 0.31	3.66 ± 0.36 (0.59)
1b	5.07	49.51 ± 0.27	0.08 ± 0.01 (0.63)
1c	5.95	69.08 ± 0.40	0.04 ± 0.02 (1.04)
1d	3.93	24.58 ± 0.37	3.35 ± 0.69 (0.81)

[a] Clog *P*: Log *P* values were computed using the Marvin Sketch 17.27 program. [b] Binding constant (K_a) values were calculated by monitoring the changes in chemical shifts of both N–H_a and N–H_b protons using the BindFit v0.5 program. [c] EC_{50} values were calculated using the modified Hill equation, n = Hill coefficient.

solvent, respectively. The difference in K_a values of compound **1c** could be due to the competition of DMSO with TBACl in Cl^- ion recognition.

The ion transport activities of compounds **1a–1d** and **2** were evaluated by fluorescence assay using model large unilamellar vesicles (LUVs). The pH-sensitive ratiometric fluorophore, 8-hydroxypyrene-1,3,6-trisulfonate (HPTS, pK_a = 7.3), was encapsulated within the LUVs of egg-yolk phosphatidylcholine (EYPC) and cholesterol (CHOL) lipids with an internal and external pH value of 7.2. The transmembrane ion transport activities of the compounds were measured by applying a pH gradient with the addition of NaOH in the extravesicular buffer (pH_{in} = 7.2, pH_{out} = 7.8).[7–10,19,22] The alteration of internal pH in the presence of compounds was examined by the change in the fluorescence intensity of HPTS at 510 nm (λ_{ex} = 450 nm). The initial screening revealed that compounds **1b** and **1c** efficiently transported Cl^- ions across the lipid bilayer (Fig. 2A). Compounds **1a–1d** showed very similar Cl^- ion binding capabilities in DMSO-d_6 solvent but compounds **1b** and **1c** showed higher Cl^- ion transport abilities compared to **1a** and **1d**, which could be due to the difference in their lipophilicity (log *P* values <5 for compounds **1a** and **1d**), which is considered as one of the essential criteria for their effective permeability across biological membranes and transmembrane Cl^- ion transport ability (Table 1). The poor Cl^- ion transport efficiency of the sulfonium-based compound **2** could be due to its higher aqueous solubility. The dose-dependent HPTS assay showed that compounds **1b** and **1c** have over 45- and 88-fold higher Cl^- ion transport efficacy than compounds **1a** and **1d**, respectively, under similar experimental conditions (Fig. S6–9†). The Hill analysis revealed that the effective concentration at 50% (EC_{50}) Cl^- ion transport activity was 79.45 and 37.98 nM for compounds **1b** and **1c**, respectively (Table 1). Accordingly, the HPTS assay revealed that compound **1c** has higher Cl^- ion transport ability than the other synthesized compounds. Consequently, further biophysical studies were carried out with compound **1c** and its derivatives.

To examine the role of other anions or cations in the Cl^- ion transport activity of compound **1c**, the HPTS assay was conducted in the presence of a pH gradient (pH_{in} = 7.2, pH_{out} = 7.8) across EYPC/CHOL-LUV ⊃ HPTS.[7–10,19,22] A substantial variance in the extent of anion transport abilities of compound **1c** (Fig. 2B) was observed when the ion transport activity was measured with intravesicular NaCl and an iso-osmolar extravesicular NaX salt (Cl^-, Br^-, I^-, F^-, and SCN^-). Although the use of intravesicular NaCl and an iso-osmolar extravesicular M^+/Cl^- salt (M^+ = Li^+, Na^+, K^+, Rb^+, and Cs^+) led to comparable Cl^- ion transport efficiencies, their pattern of Cl^- ion transport properties could be different (Fig. S10†). The outcome of the ion transport selectivity experiments revealed that the compound has Cl^- ion transport selectivity over the other investigated anions. However, the tested metal cations may not play any significant role in the ion transport process.

The HPTS assay in the absence and presence of 4-(trifluoromethoxy)phenylhydrazone (FCCP; a protonophore) and valinomycin (a selective K^+ transporter) was also performed to obtain direct experimental evidence of the preferential Cl^- ion transport mechanism of the potent compound.[7–10,19,22] An increase in the Cl^- ion transport rate in the presence of FCCP suggests a cooperative effect between the compound and FCCP, eliminating the possibility of H^+ ion transport by the compound (Fig. 3A). Similarly, the HPTS assay was also performed in the absence and presence of valinomycin. The valinomycin-mediated transport of K^+ ions from the extravesicular to intravesicular solution could induce the efflux of Cl^- ions and/or influx of OH^- ions to maintain the pH gradient. A substantial improvement in the Cl^- ion transport in the presence of valinomycin suggests the OH^-/Cl^- antiport mechanism (Fig. 3B).

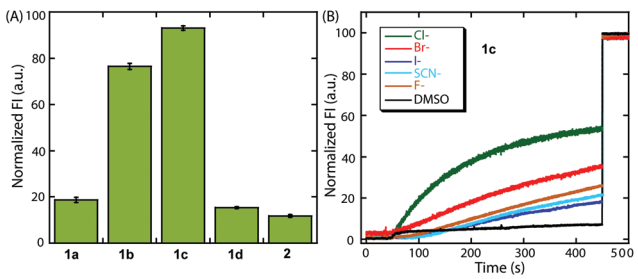

Fig. 2 Transmembrane Cl^- ion transport activity of the compounds (**1a–d** and **2**) across EYPC/CHOL-LUV ⊃ HPTS by applying a pH gradient (A; pH_i = 7.2 and pH_{out} = 7.8). The compound concentration was 0.038 μM. Anion transport selectivity of compound **1c** (B) under similar experimental conditions.

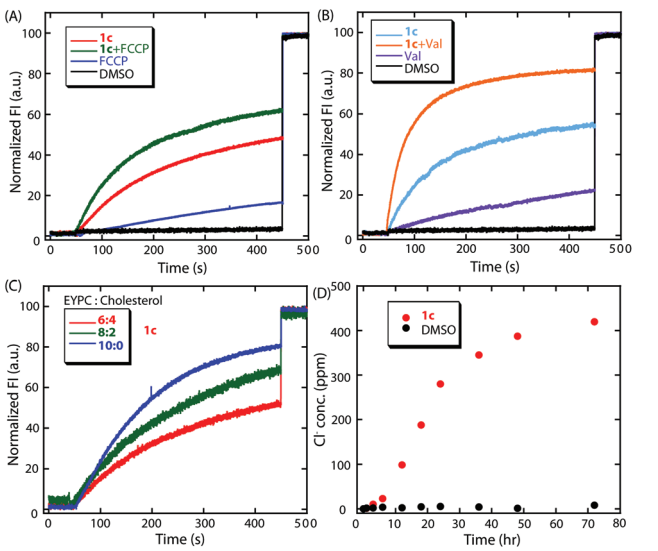

Fig. 3 Assessment of the ion transport activity of compound **1c** (0.038 μM) in the absence and presence of FCCP (4 μM) (A) and valinomycin (Val; 2.5 pM) (B). A pH gradient (pH_{in} = 7.2, pH_{out} = 7.8) was applied to initiate the transport of Cl^- ions. The effect of the cholesterol concentration on the transport of Cl^- ions in the presence of compound **1c** (0.038 μM) (C). The molar ratios of EYPC and cholesterol were varied as 6 : 4, 8 : 2, and 10 : 0 to study the effect of cholesterol on the Cl^- ion transport activity of the compounds. The Cl^- ion transport efficacy of compound **1c** (2 mM) was recorded across a U-tube by utilizing the Cl^- ion gradient, using a chloride ion-selective electrode (D).

The cooperative effect of compound **1c** and valinomycin suggests the preferential transport of OH^- ions over Cl^- ions. In the meantime, the cholesterol concentration-dependent transport (Fig. 3C) and U-tube assay (Fig. 3D) established that compound **1c** transports Cl^- ions *via* a carrier pathway.

The stimuli-mediated dealkylation ability of proanionophore **2** was investigated by HPLC and NMR analyses in the absence and presence of GSH, ROS, and light. The GSH and ROS mediated dealkylation of water-soluble proanionophore **2**, and the *in situ* production of the active ion carrier **1c** was investigated by HPLC analysis (Fig. 4A–C). The water solubility of compound **2** was 2.8 mg mL^{-1}. However, to avoid any solvent effect on the transport efficiency, all compounds (including compound **2**) were initially dissolved in DMSO and then diluted in buffer (so that the final DMSO concentration is less than 3% (v/v)). The dealkylation of proanionophore **2** (1 mmol) was performed in the presence of GSH (2 mM) in 10 mM PBS (pH 7.4) at 37 °C. HPLC analysis revealed the time-dependent dealkylation of proanionophore **2** and the regeneration of the active hydrophobic carrier **1c** along with intermediate **3** in the presence of GSH. Similarly, the dealkylation of proanionophore **2** (1 mmol) was performed in the presence of Fenton's reagent (1 mM Fe^{2+} and 5 mM H_2O_2) in 10 mM PBS (pH 7.4) at 37 °C. The time-dependent dealkylation of proanionophore **2** and the regeneration of the active hydrophobic carrier **1c** along with intermediate **4** in the presence of Fenton's reagent were analyzed by HPLC. HRMS analyses further confirmed the generation of intermediates **3** and **4** and the active anionophore **1c** (Fig. S12 and 13†). The photolytic conversion of proanionophore **2** to the active carrier **1c** was investigated by ^1H NMR in DMSO-d_6 solvent (Fig. 4D and E). The solution was irradiated using LED lamps (365 nm wavelength) for 10 min. The presence of a new signal at δ = 10.6 ppm that corresponds to the aldehyde proton indicates the release of 4-formyl-3-nitrosobenzoic acid and regeneration of compound **1c** from **2**. The photolytic generation of 4-formyl-3-nitrosobenzoic acid was also confirmed by FT-IR and HRMS analyses (Fig. S14 and 15†).

The successful regeneration of the active lipophilic carrier **1c** from water-soluble proanionophore **2** in the presence of GSH, ROS, and light encouraged us to study stimuli-activated transmembrane ion transport efficiency.[19] The time-dependent improvement of the Cl^- ion transport ability also proved the generation of the active carrier **1c** in the presence of GSH, ROS, and light (Fig. 5). Upon photo-irradiation, the rate of dealkylation was quite faster in comparison with those in the presence of GSH and ROS, which is advantageous for their bio-applicability. The photo-activated strategy can be applied for only surface phenomena due to the lack of tissue penetration ability of light. The higher levels of intracellular GSH and ROS in cancer cells could be sufficient enough to release the active carrier and promote ion transport mediated apopto-

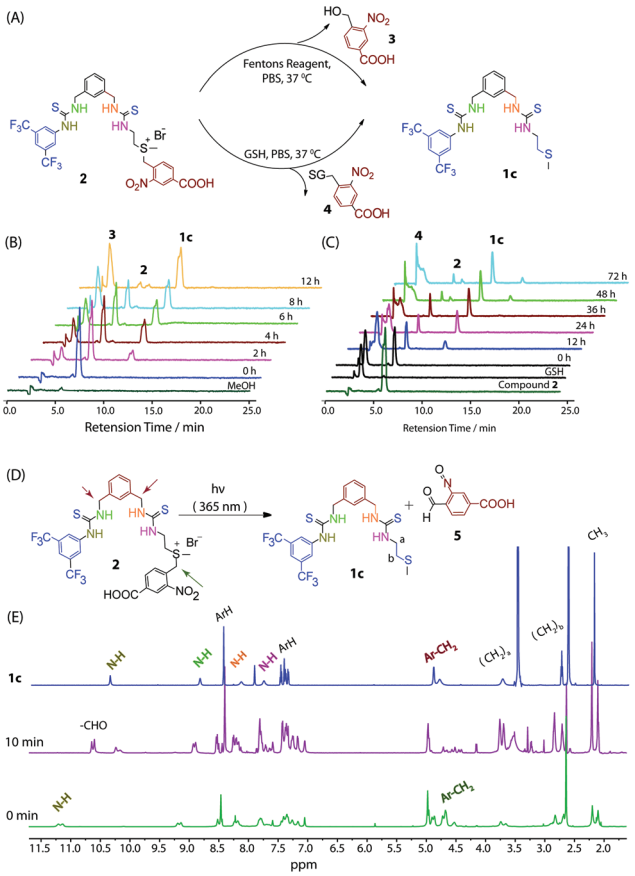

Fig. 4 Proposed mechanisms of the ROS and GSH mediated cleavage of proanionophore **2** (A). HPLC traces at different time intervals in the absence and presence of Fenton's reagent (B) and GSH (C). Proposed mechanism of the photo-mediated cleavage of proanionophore **2** (D). ^1H NMR spectra of proanionophore **2** at different time intervals (E).

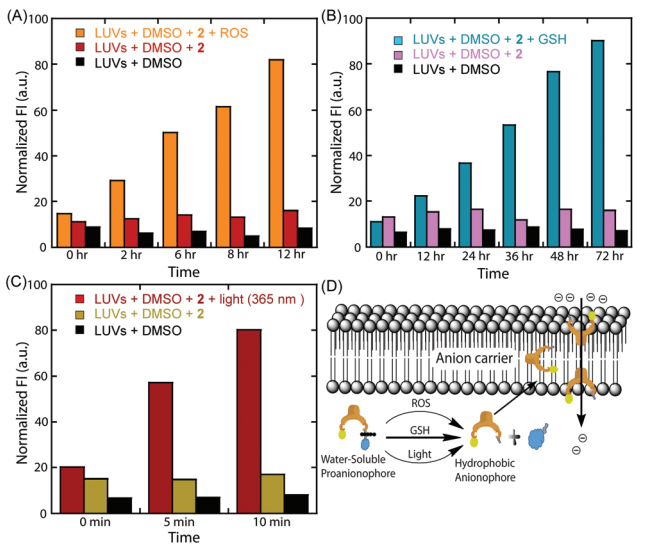

Fig. 5 Chloride ion transport measurement of the Fenton's reagent (A), glutathione (B) and light (365 nm) (C) mediated release of the active transporter **1c** from proanionophore **2** in the presence of LUVs. Schematic diagram representing the stimuli-mediated regeneration of the active anionophore from its proanionophore and its transmembrane anion transport properties (D).

sis. However, the structural integrity of proanionophore **2** was intact in the absence of GSH, ROS, and light.

Conclusions

Herein, we demonstrated a multistimuli-responsive approach to regenerate an active lipophilic ionophore from a water-soluble proanionophore. The sulfonium-based proanionophore was successfully cleaved in the presence of stimuli such as ROS, GSH, and light. ^{1}H NMR titration experiments confirmed the binding of the dithiourea derivative to the Cl^- ion. The fluorescence-based assay confirmed that the dithiourea derivative selectively transports Cl^- ions across the lipid bilayer. The U-tube and cholesterol concentration-dependent assays suggest the transport of Cl^- ions *via* a carrier pathway. The FCCP and valinomycin assays showed that the Cl^-/OH^- antiport mechanism is the operative pathway for Cl^- ion transport. The regenerated active carrier also successfully transports Cl^- ions under similar experimental conditions. Overall, this investigation revealed that the multistimuli-responsive strategy could be applied for the treatment of ion transport associated diseases.

Experimental section

Synthesis of compounds

Synthesis of 1,3-bis(isothiocyanatomethyl)benzene. The compound 1,3-bis(isothiocyanatomethyl)benzene was synthesized according to the literature procedure.[19] In brief, to a stirring solution of 1,3-phenylenedimethanamine (500 mg, 3.67 mmol) and *N*,*N*'-dicyclohexylcarbodiimide (DCC; 1.5 g) in dry THF, CS_2 (2.3 mL, 36 mmol) was added dropwise at room temperature under a N_2 atmosphere. The reaction mixture was allowed to stir for 30 min at room temperature, and the progress of the reaction was monitored by thin-layer chromatography (TLC) analysis. After this, the reaction mixture was filtered through filter paper. The filtrate was concentrated under reduced pressure. Then the crude reaction mixture was purified through column chromatography with a solvent gradient system using ethyl acetate/hexane (0–10%) to furnish the target compound as a yellowish liquid (70% yield). The compound was characterized by ^{1}H NMR and ^{13}C NMR analysis. ^{1}H NMR (600 MHz, $CDCl_3$): δ 7.34–7.30 (m, 1H), 7.21–7.19 (m, 2H), 7.15 (s, 1H), 4.64 (s, 4H); ^{13}C NMR (151 MHz, $CDCl_3$): δ 129.9, 127.6, 124.4, 121.6, 120.0, 43.2.

Synthesis of 1-(3-(isothiocyanatomethyl)benzyl)-3-(2-(methylthio)ethyl)thiourea. The compound 1-(3-(isothiocyanatomethyl)benzyl)-3-(2-(methylthio)ethyl)thiourea was synthesized according to the literature procedure.[19] In brief, to a stirring solution of 1,3-bis(isothiocyanatomethyl)benzene (500 mg, 2.27 mmol) in dry CH_3CN was added 2-(methylthio)ethan-1-amine (186.2 mg, 2.04 mmol) at room temperature under a N_2 atmosphere. Then the reaction mixture was allowed to stir for 5–6 h at room temperature, and the progress of the reaction was monitored by TLC analysis. After the completion of the reaction, the mixture was concentrate under reduced pressure. Then the crude reaction mixture was purified through column chromatography with a solvent gradient system using ethyl acetate/hexane (0–10%) to give the target compound as a white solid (90% yield). The compound was characterized by ^{1}H NMR and ^{13}C NMR analysis. ^{1}H NMR (600 MHz, $CDCl_3$): δ 7.32–7.28 (m, 1H), 7.24–7.22 (m, 1H), 7.19–7.17 (m, 2H), 4.64 (m, 2H), 4.57 (s, 2H), 3.67–3.62 (m, 2H), 2.63–2.60 (m, 2H), 1.98 (s, 3H); ^{13}C NMR (151 MHz, $CDCl_3$): δ 182.2, 135.0, 129.6, 126.4, 126.0, 48.6, 47.8, 42.7, 33.3, 14.9.

Synthesis of bis(thiourea) derivatives. To a stirring solution of 1-(3-(isothiocyanatomethyl)benzyl)-3-(2-(methylthio)ethyl) thiourea (200 mg, 0.64 mmol) in dry DMF, the corresponding aromatic amine (0.77 mmol) and triethylamine (89 mL, 0.64 mmol) were added at room temperature under a N_2 atmosphere. Then, the reaction mixture was stirred for 16–22 h at room temperature, and the reaction was monitored by TLC analysis. After the completion of the reaction, the DMF was removed through ethyl acetate/ice water workup (minimum five times) using a 100 mL separating funnel. The collected organic layers were dried over anhydrous Na_2SO_4, filtered, and concentrated under reduced pressure. The crude reaction mixture was purified through column chromatography with a solvent gradient system using ethyl acetate/hexane (0–10%) to give the corresponding yellowish compound. For compounds **1a**, **1b**, **1c**, and **1d**, the yields were 90%, 85%, 80%, and 95% respectively.

Synthesis of the sulfonium derivative (2). To a stirring solution of compound **1c** (200 mg, 0.37 mmol) in dry CH_3CN was added 4-bromomethyl-3-nitrobenzoic acid (106 mg, 0.41 mmol) at room temperature under a N_2 atmosphere. Then, the reaction mixture was stirred for 24 h under dark conditions. The progress of the reaction was monitored by TLC analysis. After the completion of the reaction, the solvent was removed under reduced pressure. The crude product was purified by preparative HPLC using the solvent system of water/methanol (0–95%) to give the yellowish solid compound **2** (70% yield).

Characterization of the synthesized compounds

1-(3-((3-(2-(Methylthio)ethyl)thioureido)methyl)benzyl)-3-phenylthiourea (1a). The general procedure as mentioned in the earlier section was followed, using 1-(3-(isothiocyanatomethyl)benzyl)-3-(2-(methylthio)ethyl)thiourea (200 mg, 0.64 mmol), aniline (71.15 mg, 0.77 mmol) and triethylamine (89 mL, 0.64 mmol). The yellowish compound was isolated in 90% yield. The compound was characterized by HRMS (ESI), ^{1}H NMR and ^{13}C NMR analysis. ^{1}H NMR (600 MHz, DMSO-d_6): δ 9.61 (s, 1H), 8.14 (s, 1H), 7.98 (s, 1H), 7.60 (s, 1H), 7.74–7.43 (m, 2H), 7.35–7.32 (m, 2H), 7.31–7.29 (m, 1H), 7.25 (s, 1H), 7.23–7.22 (m, 1H), 7.19–7.17 (m, 1H), 7.14–7.11 (m, 1H), 4.73–4.66 (m, 4H), 3.61 (m, 2H), 2.64–2.62 (t, J = 7.0 Hz, 2H), 2.08 (s, 3H); ^{13}C NMR (151 MHz, $CDCl_3$): δ 181.3, 139.6, 139.4, 129.4, 128.7, 126.8, 126.5, 126.4, 124.8, 123.8, 47.8, 43.3, 32.93,

15.1; HRMS (ESI) *m*/*z*: calculated for $C_{19}H_{24}N_4S_3$ $(M + H)^+$: 405.1236, found: 405.1236.

1-(3-((3-(2-(Methylthio)ethyl)thioureido)methyl)benzyl)-3-(4-(trifluoromethyl)phenyl)thiourea (1b). The general procedure as mentioned in the earlier section was followed, using 1-(3-(isothiocyanatomethyl)benzyl)-3-(2-(methylthio) ethyl)thiourea (200 mg, 0.64 mmol), 4-(trifluoromethyl)aniline (124.07 mg, 0.77 mmol) and triethylamine (89 mL, 0.64 mmol). The crude yellowish compound was isolated in 85% yield. The compound was characterized by the HRMS (ESI), ^{1}H NMR and ^{13}C NMR analysis. ^{1}H NMR (600 MHz, DMSO-d_6): δ 9.97 (s, 1H), 8.47 (s, 1H), 8.00 (s, 1H), 7.75–7.73 (m, 2H), 7.68–7.66 (m, 2H), 7.6 (s, 1H), 7.33–7.30 (m, 1H), 7.26 (s, 1H), 7.24–7.23 (m, 1H), 7.20–7.19 (m, 1H), 4.74–4.67 (m, 4 H), 3.61 (m, 2H), 2.63–2.61 (t, J = 7.0 Hz, 2H), 2.08 (s, 3H); ^{13}C NMR (151 MHz, $CDCl_3$): δ 182.4, 181.0, 140.8, 137.9, 129.1, 126.8, 126.7, 126.0, 124.8, 122.9, 122.5, 121.2, 48.3, 48.1, 42.9, 32.9, 14.9; HRMS (ESI) *m*/*z*: calculated for $C_{20}H_{23}F_3N_4S_3$ $(M + H)^+$: 473.1110, found: 473.1110.

1-(3,5-Bis(trifluoromethyl)phenyl)-3-(3-((3-(2-(methylthio)-ethyl)thioureido)methyl)benzyl)thiourea (1c). The general procedure as mentioned in the earlier section was followed, using 1-(3-(isothiocyanatomethyl)benzyl)-3-(2-(methylthio) ethyl)thiourea (200 mg, 0.64 mmol), 3,5-bis(trifluoromethyl) aniline (416.26 mg, 0.77 mmol) and triethylamine (89 mL, 0.64 mmol). The crude yellowish compound was isolated in 90% yield. The compound was characterized by the ES-MS, ^{1}H NMR and ^{13}C NMR analysis. ^{1}H NMR (600 MHz, DMSO-d_6): δ 10.17 (s, 1H), 8.67 (s, 1H), 8.28 (s, 2H), 7.98 (s, 1H), 7.76 (s, 1H), 7.60 (s, 1H), 7.56–7.31 (t, J = 7.6 Hz, 1H), 7.26 (s, 1H), 7.25–7.23 (m, 1H), 7.20–7.19 (m, 1H), 4.77–4.66 (m, 4H), 3.61 (m, 2H), 2.63–2.61 (t, 2H), 2.07 (s, 3H); ^{13}C NMR (151 MHz, $CDCl_3$): δ 181.3, 139.8, 131.8, 131.6, 129.1, 126.9, 126.8, 123.8, 122.0, 121.9, 120.2, 118.1, 50.9, 48.2, 42.9, 32.9, 14.6; HRMS (ESI) *m*/*z*: calculated for $C_{29}H_{22}F_6N_4O_4S_3$ $(M + H)^+$: 541.0984, found: 541.0961.

1-(4-Methoxyphenyl)-3-(3-((3-(2-(methylthio)ethyl)thioureido)methyl)benzyl)thiourea (1d). The general procedure as mentioned in the earlier section was followed, using 1-(3-(isothiocyanatomethyl)benzyl)-3-(2-(methylthio)ethyl)thiourea (200 mg, 0.64 mmol), 4-methoxyaniline (94.89 mg, 0.77 mmol) and triethylamine (89 mL, 0.64 mmol). The crude yellowish compound was isolated in 95% yield. The compound was characterized by the ES-MS, ^{1}H NMR and ^{13}C NMR analysis. ^{1}H NMR (600 MHz, DMSO-d6): δ 9.46 (s, 1H), 8.01 (s, 1H), 7.96 (s, 1H), 7.62 (s, 1H), 7.30–7.28 (m, 1H), 7.26–7.24 (m, 2H), 7.22 (s, 1H), 7.20–7.19 (m, 1H), 7.17–7.16 (m, 1H), 6.92–6.90 (m, 2H), 4.70–4.69 (m, 4H), 3.74 (s, 3H), 2.64–2.62 (m, 2H), 2.08 (s, 3H); ^{13}C NMR (151 MHz, $CDCl_3$): δ 182.3, 181.5, 158.9, 138.3, 137.8, 129.6, 128.4, 127.6, 126.9, 126.7, 126.0, 115.3, 55.6, 48.8, 48.1, 42.9, 33.3, 14.9; HRMS (ESI) *m*/*z*: calculated for $C_{20}H_{26}N_4OS_3$ $(M + H)^+$: 435.1342, found: 435.1316.

(2-(3-(3-((3-(3,5-Bis(trifluoromethyl)phenyl)thioureido)methyl)-benzyl)thioureido)ethyl)(4-carboxy-2-nitrobenzyl)(methyl)-sulfonium bromide (2). The general procedure as mentioned in the earlier section was followed, using 1c (200 mg, 0.37 mmol) and 4-bromomethyl-3-nitrobenzoic acid (106 mg, 0.41 mmol). The crude compound was isolated in 70% yield. The compound was characterized by ES-MS, ^{1}H NMR and ^{13}C NMR analysis. ^{1}H NMR (600 MHz, DMSO-d_6): δ 11.15–11.08 (m, 1H), 9.13–9.07 (m, 1H), 8.44 (s, 1H), 8.39–8.37 (m, 2H), 8.14–8.10 (m, 1H), 7.74–7.70 (m, 1H), 7.51 (s, 1H), 7.36–7.27 (m, 3H), 7.17 (s, 1H), 7.08 (s, 1H), 6.96 (s, 1H), 4.87–4.84 (m, 2H), 4.79–4.75 (m, 2H), 4.61–4.56 (m, 2H), 3.62–3.54 (m, 2H), 2.69 (m, 2H), 2.06 (s, 3H); ^{13}C NMR (151 MHz, $CDCl_3$): δ 181.4, 165.7, 163.6, 148.2, 142.6, 134.6, 133.2, 132.6, 130.6, 129.0, 127.1, 126.3, 126.0, 124.6, 123.1, 122.8, 121.5, 116.4, 47.0, 46.2, 43.7, 32.1, 31.6, 15.2; HRMS (ESI) *m*/*z*: calculated for $C_{29}H_{28}F_6N_5O_4S_3^+$ (M): 720.1280, found: 720.1249.

Measurement of anion recognition, anion transport, and regeneration activities

The detailed experimental procedures for anion recognition, chloride ion transport, U-tube assay, vesicle leakage, and other biophysical assays are described in the ESI.†

Conflicts of interest

There are no conflicts to declare.

Acknowledgements

The authors gratefully acknowledge the Department of Biotechnology, Government of India (MED/2015/04) and the Science and Engineering Research Board, Government of India (EMR/2016/005008) for financial support.

References

1 K. Fernald and M. Kurokawa, *Trends Cell Biol.*, 2013, **23**, 620–633.
2 V. Labi and M. Erlacher, *Cell Death Dis.*, 2015, **6**, 1675.
3 S. Fulda, *Int. J. Cell Biol.*, 2010, **2010**, 370835.
4 N. Akhtar, N. Pradhan, G. K. Barik, S. Chatterjee, S. Ghosh, A. Saha, P. Satpati, A. Bhattacharyya, M. K. Santra and D. Manna, *ACS Appl. Mater. Interfaces*, 2020, **12**, 25521–25533.
5 N. Akhtar, O. Biswas and D. Manna, *Chem. Commun.*, 2020, DOI: 10.1039/D0CC05489E.
6 A. Bansal and M. C. Simon, *J. Cell Biol.*, 2018, **217**, 2291–2298.
7 N. Akhtar, A. Saha, V. Kumar, N. Pradhan, S. Panda, S. Morla, S. Kumar and D. Manna, *ACS Appl. Mater. Interfaces*, 2018, **10**, 33803–33813.
8 T. Saha, M. S. Hossain, D. Saha, M. Lahiri and P. Talukdar, *J. Am. Chem. Soc.*, 2016, **138**, 7558–7567.
9 S. B. Salunke, J. A. Malla and P. Talukdar, *Angew. Chem., Int. Ed.*, 2019, **58**, 5354–5358.
10 S. V. Shinde and P. Talukdar, *Org. Biomol. Chem.*, 2019, **17**, 4483–4490.

11 E. N. W. Howe and P. A. Gale, *J. Am. Chem. Soc.*, 2019, **141**, 10654–10660.
12 H. Li, H. Valkenier, A. G. Thorne, C. M. Dias, J. A. Cooper, M. Kieffer, N. Busschaert, P. A. Gale, D. N. Sheppard and A. P. Davis, *Chem. Sci.*, 2019, **10**, 9663–9672.
13 R. Montis, A. Bencini, S. J. Coles, L. Conti, L. Fusaro, P. A. Gale, C. Giorgi, P. N. Horton, V. Lippolis, L. K. Mapp and C. Caltagirone, *Chem. Commun.*, 2019, **55**, 2745–2748.
14 M. J. Spooner, H. Li, I. Marques, P. M. R. Costa, X. Wu, E. N. W. Howe, N. Busschaert, S. J. Moore, M. E. Light, D. N. Sheppard, V. Felix and P. A. Gale, *Chem. Sci.*, 2019, **10**, 1976–1985.
15 X. Wu, J. R. Small, A. Cataldo, A. M. Withecombe, P. Turner and P. A. Gale, *Angew. Chem., Int. Ed.*, 2019, **58**, 15142–15147.
16 S. Zhang, Y. Wang, W. Xie, E. N. W. Howe, N. Busschaert, A. Sauvat, M. Leduc, L. C. Gomes-da-Silva, G. Chen, I. Martins, X. Deng, L. Maiuri, O. Kepp, T. Soussi, P. A. Gale, N. Zamzami and G. Kroemer, *Cell Death Dis.*, 2019, **10**, 242.
17 O. Biswas, N. Akhtar, Y. Vashi, A. Saha, V. Kumar, S. Pal, S. Kumar and D. Manna, *ACS Appl. Bio Mater.*, 2020, **3**, 935–944.
18 A. Saha, N. Akhtar, V. Kumar, S. Kumar, H. K. Srivastava, S. Kumar and D. Manna, *Org. Biomol. Chem.*, 2019, **17**, 5779–5788.
19 N. Akhtar, N. Pradhan, A. Saha, V. Kumar, O. Biswas, S. Dey, M. Shah, S. Kumar and D. Manna, *Chem. Commun.*, 2019, **55**, 8482–8485.
20 B. Díaz de Greñu, P. I. Hernández, M. Espona, D. Quiñonero, M. E. Light, T. Torroba, R. Pérez-Tomás and R. Quesada, *Chem*, 2011, **17**, 14074–14083.
21 S. Cournoyer, A. Addioui, A. Belounis, M. Beaunoyer, C. Nyalendo, R. Le Gall, P. Teira, E. Haddad, G. Vassal and H. Sartelet, *BMC Cancer*, 2019, **19**, 1018.
22 J. A. Malla, R. M. Umesh, S. Yousf, S. Mane, S. Sharma, M. Lahiri and P. Talukdar, *Angew. Chem., Int. Ed.*, 2020, **59**, 7944–7952.
23 M. A. Inlay, V. Choe, S. Bharathi, N. B. Fernhoff, J. R. Baker Jr., I. L. Weissman and S. K. Choi, *Chem. Commun.*, 2013, **49**, 4971–4973.
24 C. Fowley, N. Nomikou, A. P. McHale, B. McCaughan and J. F. Callan, *Chem. Commun.*, 2013, **49**, 8934–8936.
25 S. Dey, A. Patel, K. Raina, N. Pradhan, O. Biswas, R. P. Thummer and D. Manna, *Chem. Commun.*, 2020, **56**, 1661–1664.
26 D. Wang, M. Yu, N. Liu, C. Lian, Z. Hou, R. Wang, R. Zhao, W. Li, Y. Jiang, X. Shi, S. Li, F. Yin and Z. Li, *Chem. Sci.*, 2019, **10**, 4966–4972.
27 R. Nathani, P. Moody, M. E. Smith, R. J. Fitzmaurice and S. Caddick, *ChemBioChem*, 2012, **13**, 1283–1285.